

Critical Temperature of Axially Loaded Steel Members with Wide-Flange Shapes Exposed to Fire

ANA SAUCA, RACHEL CHICCHI, CHAO ZHANG, and LISA CHOE

ABSTRACT

This paper presents closed-form equations that were developed to evaluate critical temperatures of structural steel compression and tension members exposed to fire. The deterministic approach involved a parametric study using finite element simulations in order to identify influencing factors—for example, mechanical properties of steel, member slenderness, and axial load ratios. Statistical models were employed to develop closed-form equations representing the best fit of numerical results. A comparison with experimental column test data indicates that the proposed equation for compression members provides a conservative lower bound (16% lower on average) relative to the test data at load ratios greater than 0.3. A sensitivity study was also performed to further explore uncertainty in predicted critical temperatures due to variability of axial load ratios. For both compression and tension members, the ambient-temperature yield stress of steel, F_y , has a great impact on determination of axial load ratios, subsequently influencing the overall accuracy of the critical temperature estimated by the proposed equations. The applicability of the proposed equations is limited to wide-flange steel members that are simply supported, concentrically loaded, and exposed to uniform heating.

Keywords: critical temperature, structural steel, compression, tension, fire.

INTRODUCTION

Background

In the United States, fire resistance design of load-carrying steel members (beams and columns) in steel-framed buildings is mainly achieved through compliance with prescriptive provisions in the International Building Code (ICC, 2009). In this approach, fireproofing insulation is applied to exposed steel so that the steel does not exceed the critical temperature under standard fire conditions for a minimum specified duration (known as a fire-resistant rating). According to the American Society for Testing and Materials (ASTM) E119 standard (ASTM, 2019), the critical temperature of exposed steel members in a standard fire test is 1000°F (538°C) for columns and 1100°F (593°C) for beams, determined as the average temperature of all measurement points. However, these limiting temperatures seldom account for the effects of imposed load

levels, semi-rigid support conditions, and both member and section slenderness.

Prescriptive methods have provided little information regarding the high-temperature strength and associated failure modes of steel members exposed to fire. As an alternative engineering approach, AISC *Specification* Appendix 4 (AISC, 2016b) provides high-temperature member strength equations for the limit states of flexural buckling and lateral-torsional buckling. To calculate member strengths at elevated temperature, users need to define the temperature of interest as an input, which must be greater than 392°F (200°C), based on heat transfer analyses or engineering judgments. These equations are less practical for solving the critical temperature at which the member demand exceeds its capacity because iteration with increasing temperatures is required (Saucu et al., 2019).

In Europe, the evaluation of critical temperatures of axially loaded steel members was of interest beginning in the late 1970s. Kruppa (1979) defined “critical” or “collapse” temperature as the temperature at which the structure cannot assume its function and proposed a critical temperature equation for steel columns using the temperature-dependent axial stress and buckling coefficient. Rubert and Schaumann (1988) used finite element models for calculating critical temperature of steel columns. The analytical results were compared with 50 full-scale column tests and showed good correlation at temperatures in the range of 390°F (200°C) to 1300°F (700°C) and utilization (demand-to-capacity) ratios of 0.2 to 0.6.

Neves (1995) further explored the critical temperature of restrained steel columns analytically, with three column slenderness values (40, 80, and 120) and eccentricity of the

Ana Saucu, Post-doc Research Engineer, Danish Institute of Fire and Security Technology, Denmark. Email: AS@dbigroup.dk

Rachel Chicchi, Assistant Professor, University of Cincinnati, Cincinnati, Ohio. Email: rachel.chicchi@uc.edu

Chao Zhang, Guest Researcher, National Institute of Standards and Technology, Gaithersburg, Md. Email: chao.zhang@nist.gov

Lisa Choe, Research Structural Engineer, National Institute of Standards and Technology, Gaithersburg, Md. Email: lisa.choe@nist.gov (corresponding)

Paper No. 2019-21

applied load. Due to the variety of parameters being considered, a critical temperature equation was not proposed. Similarly, Franssen (2000) applied an arc-length numerical technique to calculate the collapse temperature of columns. Wang et al. (2010) evaluated the critical temperature of restrained steel columns using a finite element ABAQUS model (Smith, 2009) with two-dimensional beam elements. Their study indicated that the section geometry had very limited effects on the column critical temperature, and the critical temperature of a restrained column can be obtained by making a reduction in corresponding values of columns without axial restraint.

The European standards provide critical temperature equations or tabulated data for steel members. For steel members “without instability phenomena” (e.g., tension or flexural yielding), the critical temperature is only a function of a utilization ratio for fire conditions (CEN, 2005). This equation is very similar to an inverse of the temperature-dependent yield strength of structural steel. For steel columns, however, only tabulated forms (e.g., Vassart et al., 2014; BSI, 2005) are available to evaluate critical temperatures, depending upon the member slenderness and utilization ratio. Despite all the limitations (i.e., applicability only under standard fires, uniform distribution of temperatures across the section and length, and simplified boundary conditions), the critical temperature method would remain as a useful tool to evaluate the fire resistance of load-carrying steel members (Milke, 2016).

Objectives, Scope, and Limitations

The significance of the critical temperature method lies in its simplicity and the useful information obtained about a structural member exposed to varying temperatures during a fire event. To date, however, a critical temperature method is not available in AISC *Specification* Appendix 4 (AISC, 2016b). The objective of the study presented herein was to develop closed-form solutions that can be used to evaluate critical temperatures of axially loaded steel members exposed to fire. The methodology adopted in this study included (1) a parametric study using 900 finite element models to identify the influencing variables for determination of critical temperatures of steel members at elevated temperatures, (2) three-dimensional regression analyses to develop a closed-form equation that represents the best fit of numerical results with given ranges of the parameters considered in this study, (3) comparison of the critical temperature predicted using the proposed equation with test data in literature, and (4) a sensitivity study to estimate uncertainty in critical temperatures computed using proposed equations.

The scope of this study focused on the critical temperature of structural steel tension and compression members with wide-flange rolled shapes. The parameters influencing

critical temperatures were evaluated, including various axial load levels, steel grades, and section compactness and member slenderness at ambient temperature. The use of proposed equations presented herein should be limited to wide-flange steel members simply supported, concentrically loaded, and exposed to uniform heating. Future work will include the effects of thermal restraints as well as thermal gradients through the section depth and along the member length.

NUMERICAL ANALYSES

Test Bed

The critical temperature of axially loaded steel columns with wide-flange rolled shapes was evaluated using the finite element method (FEM). In this study, a total of 900 FEM models were analyzed in combination with various ranges of parameters summarized in Table 1. Five different wide-flange rolled shapes, including W8×31, W10×68, W14×22, W14×90, and W14×211, were used in this study. With the exception of the W14×22, all other shapes are compact for compression at ambient temperature. In addition, two American standard grades of structural steel shapes, including $F_y = 50$ ksi and $F_y = 36$ ksi, are considered, where F_y is the minimum specified yield stress. Effective slenderness ratios, L_c/r , range from 20 to 200, and applied load ratios vary from 0.1 to 0.9. The load ratio is defined as the axial demand at elevated temperatures, P_u , normalized by the nominal capacity at ambient temperature, P_{na} . The demand for fire condition can be determined from the load combination for extraordinary events, $1.2 \times$ dead load $+ 0.5 \times$ live load $+ A_T$, where A_T is the force and deformation induced by fire effects (ASCE, 2016). In this study, all investigated members were assumed to be simply supported, concentrically loaded, and exposed to uniform heating; therefore, the magnitude of A_T was assumed to be zero. The nominal capacity at ambient temperature, P_{na} , can be calculated using AISC *Specification* Section E3.

Numerical models of columns were developed using three-dimensional shell elements. Each model was discretized into 50 elements along the member length and 8 elements each for the flange and the web. The FEM solution with this element size was converged with the maximum error of about 2%, based on the mesh density study presented in Sauca et al. (2019). Linear kinematic constraints were applied to both the flanges and web at each end in order to enforce rigid planar behavior. The column ends were simply supported. An axial force was applied to the centroid of the end section. An initial displacement at midspan was taken as the 1/1000 of the column length to simulate global imperfections (initial sweep). Local geometrical imperfections were implemented by scaling a sinusoidal deformation of the cross sections using elastic buckling analyses. The

Shape	F_y	L_c/r	P_u/P_{na}
W8×31 W10×68 W14×22 W14×90 W14×211	36 ksi (250 MPa) 50 ksi (350 MPa)	20 to 200 (increment: 20)	0.1 to 0.9 (increment: 0.1)

scaled value was taken as the larger of a web out-of-flatness equal to the ratio of the section depth over 150 (Kim and Lee, 2002) or a tilt in the compression flanges taken as the ratio of the flange width over 150 (Zhang et al., 2015). No residual stresses were applied because their influence is limited at elevated temperature (Vila Real et al., 2007). The Eurocode 3 (CEN, 2005) temperature-dependent stress-strain relationship was employed, whereas no thermal creep model was incorporated explicitly.

In order to estimate critical temperatures of columns using FEM models, an axial load as a fraction of P_{na} was applied at ambient temperature, and then the member temperature was increased monotonically until force equilibriums could not be achieved. The maximum value of temperature achieved from each FEM model was defined as a critical temperature.

Numerical Results

Figure 1 shows the critical temperature, T_{cr} , of steel columns predicted using the finite element models with $F_y = 50$ ksi (350 MPa), where the dotted lines indicate the linear regression of these predicted results. Figure 1(a) shows the average critical temperature of columns as a function of a load ratio. The error bars indicate the standard deviation of the results varying with five different shapes and all slenderness ratios ($L_c/r = 20$ to 200) at the same load level. Figure 1(b) shows the relationship of the average critical temperature of all five columns versus the slenderness ratio at four different load ratios (P_u/P_{na}) of 0.1, 0.3, 0.6, and 0.9. As shown, the critical temperature appears to be linearly decreasing with both increasing load ratios and increasing slenderness ratios. However, the critical temperature is less sensitive to the member slenderness at the same load level. Some statistical results and discussions on the effect of member slenderness and applied load levels are as follows.

- *Member slenderness:* The reduction in critical temperatures with increasing slenderness ratios is influenced by the applied load level. At load ratios smaller than 0.5, the critical temperature is reduced by about 10% between the slenderness ratio of 20 and 200. At higher load ratios, the critical temperature can reduce by 30% to 60% for the L_c/r ratio of 20 to 200. This reduction is not proportional to load ratios.

- *Applied load level:* The critical temperature is affected by the magnitude of applied loads. The reduction in critical temperature can reach nearly 80% between the load ratio of 0.1 and 0.9 and 20% on average at each increment of 0.1. Larger scatter of the results is observed for the models with the load ratio between 0.5 and 0.8, as shown by the error bars in Figure 1(a), due to variation in member slenderness. The critical temperature versus applied load relationship shows a very good linear fit, similar to an empirical relationship presented in Choe et al. (2011).

Figure 2 shows critical temperatures of steel columns relative to load ratio with (1) all five shapes and two different steel grades and (2) W14×22 and W14×90 columns with $F_y = 50$ ksi. Both graphs considered the slenderness ratios of 20, 40, and 100. Some discussions on the effect of the ambient yield stress, F_y , and the section compactness are as follows.

- *Ambient yield strength:* The variation in critical temperatures predicted using two different steel grades (36 ksi versus 50 ksi) is about 1% on average. This is to be expected as the buckling behavior of columns with the slenderness ratio greater than 40 (i.e., medium-length to slender columns) is mainly affected by low strain levels (less than 0.05% strain) and temperature-dependent elastic modulus (Choe et al., 2017).
- *Section geometry:* Between two different wide-flange shapes, the variation in critical temperatures is over 10% for short columns subjected to large axial loads (i.e., a slenderness ratio less than 60 and a load ratio greater than 0.6). The critical temperature variation for slender columns subjected to small axial loads is below 5%.

PROPOSED CLOSED-FORM EQUATION

Compression Members

The numerical results from 900 finite-element models were used to develop a closed-form equation that predicts critical temperatures of steel columns as a function of member slenderness and load ratio. The three-dimensional linear polynomial model, as shown in Figure 3, was employed

based on the results from the parametric study presented previously. Equations 1 and 2 show the resulting best linear fit equation in °C and °F, respectively, with the *R*-square value of 0.97.

$$T_{cr} = 858 - 0.455 \frac{L_c}{r} - 722 \frac{P_u}{P_{na}} \quad \text{in } ^\circ\text{C} \quad (1)$$

$$T_{cr} = 1580 - 0.814 \frac{L_c}{r} - 1300 \frac{P_u}{P_{na}} \quad \text{in } ^\circ\text{F} \quad (2)$$

Figure 4 shows a comparison of critical temperatures calculated using the proposed equation with those estimated using various methods, including FEM models, the ASTM E119 limiting temperature of columns, and the AISC *Specification* Appendix 4 equation. In Figure 4(a), the results of

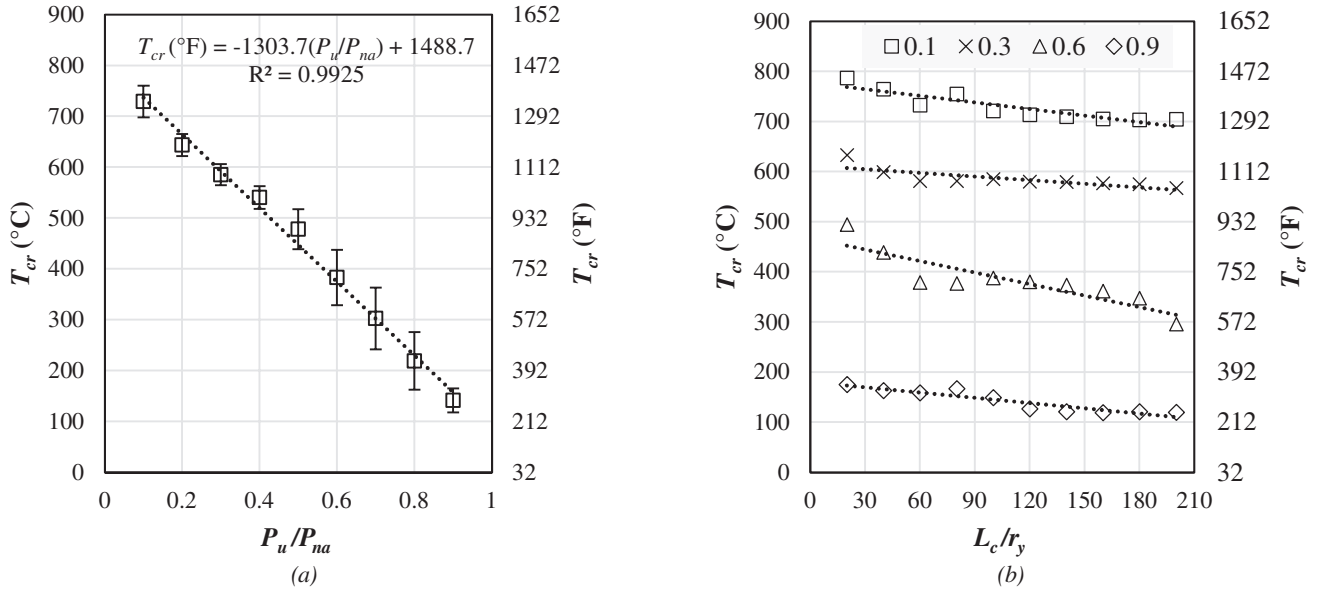


Fig. 1. Average critical temperatures for columns predicted using FEM models of five shapes with $F_y = 50$ ksi as a function of (a) load ratio (P_u/P_{na}) and (b) member slenderness (L_c/r_y).

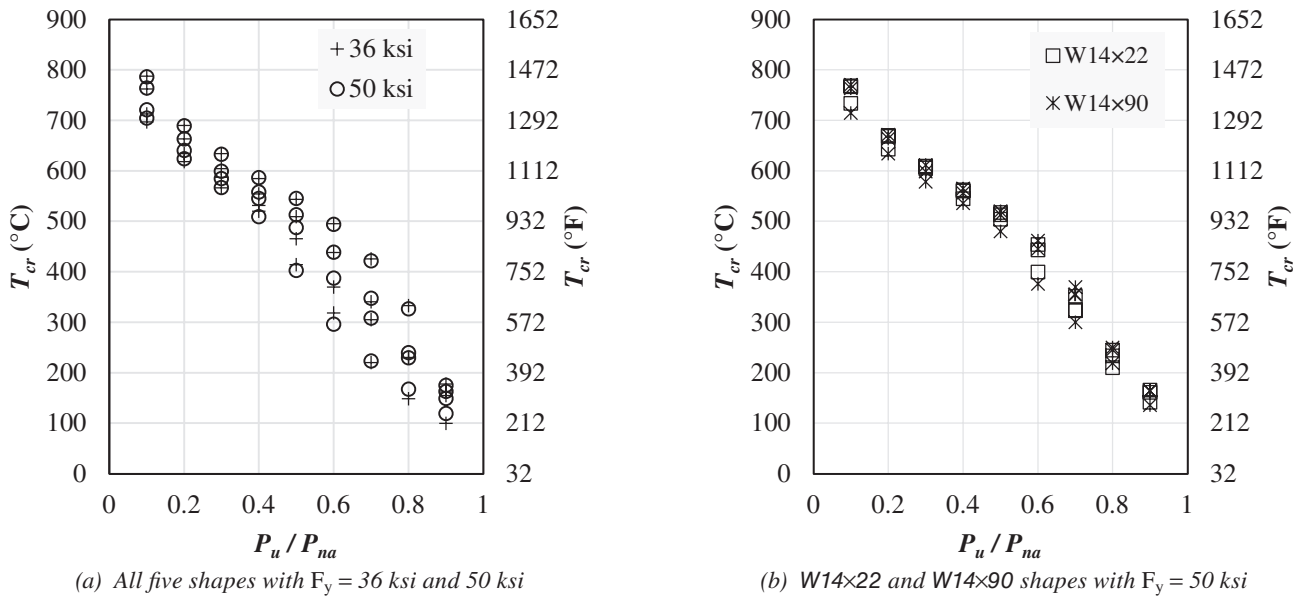


Fig. 2. Predicted critical temperatures of columns with slenderness ratios of 20, 40, and 100.

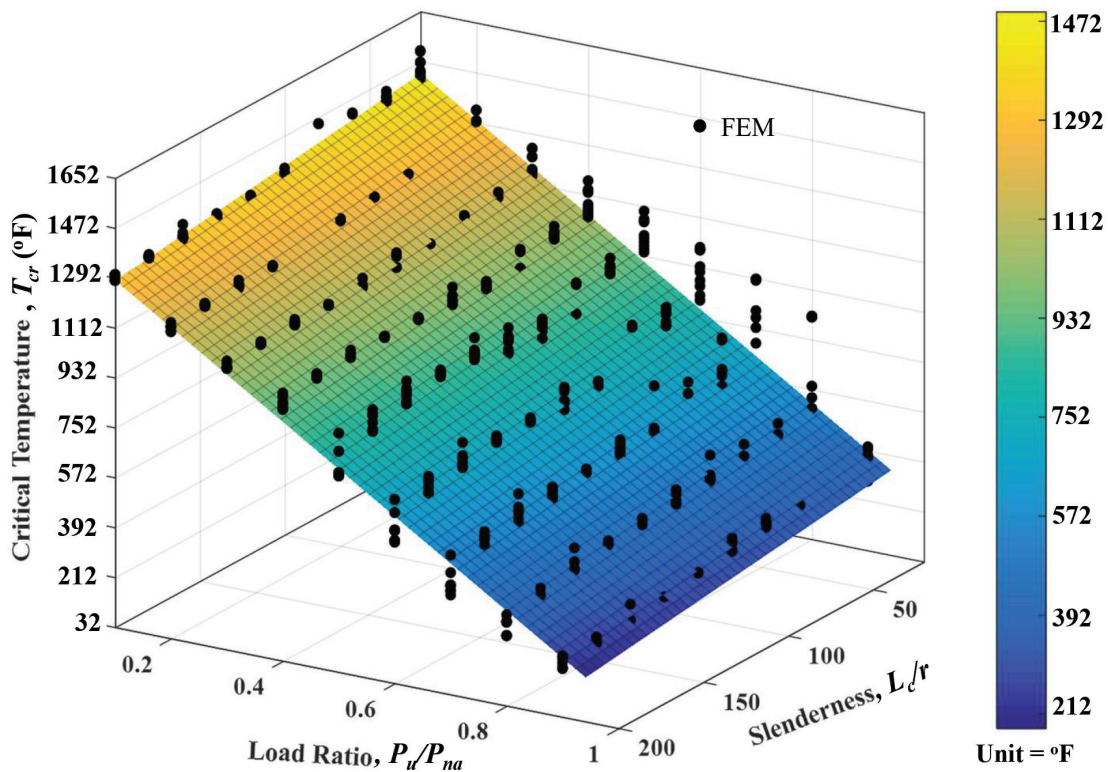
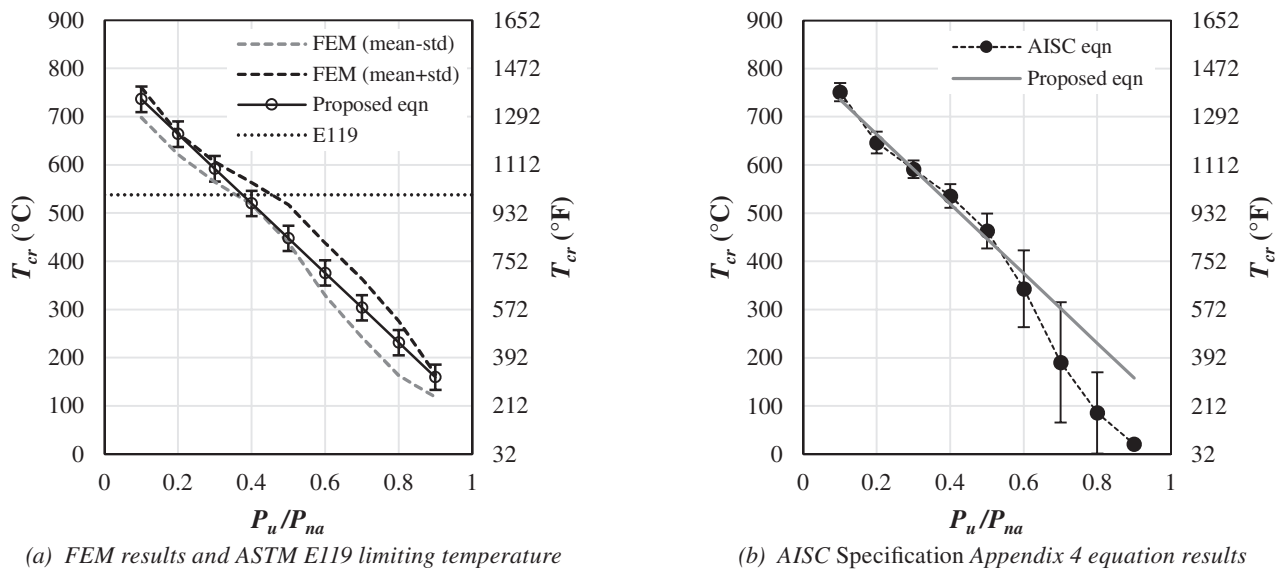


Fig. 3. A three-dimensional linear curve fit of 900 FEM models of columns.



(a) FEM results and ASTM E119 limiting temperature

(b) AISC Specification Appendix 4 equation results

Fig. 4. Comparisons of the proposed column equation.

FEM models are presented with two lines: the upper bound as mean values plus standard deviations (std) and the lower bound as mean values minus standard deviations. The standard deviation incorporates the total variation in the FEM data resulting from the range in parameters described in Table 1 at each load level. The error bars plotted with the critical temperature predicted using Equation 1 indicate the standard deviation due to slenderness ratio ranges from 20 to 200. Overall, the proposed equation compares reasonably well with the FEM results. With this equation, the load-bearing capacity of steel columns is approximately 40% of the ambient capacity at the ASTM E119 limiting temperature of 1000°F (540°C).

Figure 4(b) gives a comparison with critical temperatures estimated using the AISC *Specification* Appendix 4 flexural buckling strength equation, Equation A-4-2. A detailed description of computation methods, which required an iteration process, is presented in Sauca et al. (2019). The error bars in this figure indicate the standard deviation resulted from a variety of steel shapes and slenderness ratios considered in this study. For columns with load ratios less than 0.6, the proposed equation also adequately predicts critical temperatures, with 2% difference on average. At load ratios equal to or greater than 0.6, however, the proposed equation may overestimate critical temperatures estimated using AISC *Specification* Equation A-4-2.

The efficacy of Equation 1 was examined by comparing predicted critical temperatures with observed critical temperatures from previous experimental studies (Franssen et al., 1996; Ali et al., 1998; Choe et al., 2011) of steel columns that had similar properties used for the present study. Test data used for this comparison included 36 wide-flange, hot-rolled column specimens that had simply supported

boundary conditions and were concentrically loaded (i.e., an eccentricity of axial loading was less than the 1/1000 of the column length) at elevated temperatures. In this data set, the ambient-temperature yield stress ranged from 32 ksi (220 MPa) to 60 ksi (400 MPa), and effective slenderness ratios varied from 30 to 137.

Figure 5 shows a comparison of the column test data with predicted critical temperatures using Equation 1 and with the linear regression of the data itself. Overall, the proposed equation provides a conservative lower bound of the test results. For the specimens with load ratios greater than 0.3, the calculated critical temperatures are approximately 16% lower than the measured values on average. For load ratios less than 0.2, Equation 1 slightly overestimates the critical temperature by 4%.

Tension Members

Critical temperatures of uniformly heated steel members in tension have a dependency of high-temperature mechanical properties, such as temperature-dependent yield stress and ultimate tensile strength. This paper also suggests a critical temperature equation for tensile yielding in gross sections of a steel member as a function of imposed tension loads, T_u , at elevated temperature normalized by the nominal capacity, T_{na} , at ambient temperature. As shown in Figure 6, the critical temperature equation is an inverse relationship of the AISC *Specification* temperature-dependent retention factors for yield stress, k_y , essentially the same as the Eurocode 3 (CEN, 2005) retention factors. The logarithmic regression model was employed similar to the Eurocode 3 critical temperature equation for members “without instability phenomena.” Equations 3 and 4 show the best fit equation

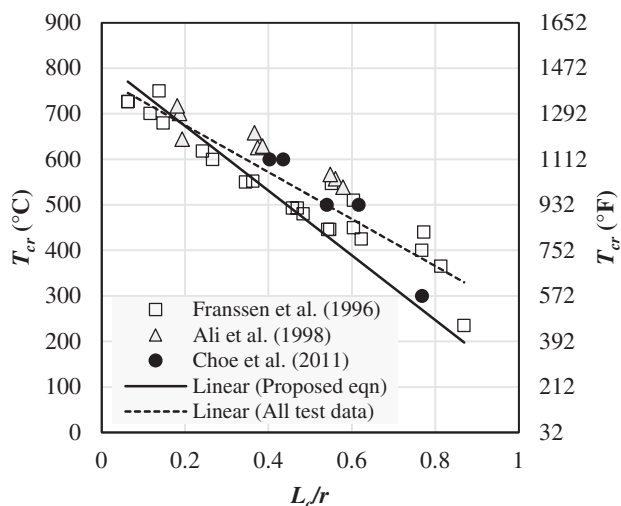


Fig. 5. A comparison of critical temperatures of columns calculated using Equation 1 with experimental test data.

Variable	Mean	CV	Std
F_y	50 ksi (350 MPa)	0.10	5 ksi (35 MPa)
E	29,000 ksi (200 GPa)	0.06	1,740 ksi (12 GPa)
DL	103% unfactored	0.10	a
LL	25% unfactored	0.60	b

a: The standard deviation for DL is taken as the mean load $\times 1.025 \times 0.10$.
b: The standard deviation for LL is taken as the mean load $\times 0.25 \times 0.60$.

in °C and °F, respectively, with the R -square value of 0.99. For the use of these equations, the load ratio, T_u/T_{na} , must be greater than or equal to 0.01.

$$T_{cr} = 435 - 170 \ln\left(\frac{T_u}{T_{na}}\right) \text{ in } ^\circ\text{C} \quad (3)$$

$$T_{cr} = 816 - 306 \ln\left(\frac{T_u}{T_{na}}\right) \text{ in } ^\circ\text{F} \quad (4)$$

ESTIMATED UNCERTAINTY OF CLOSED-FORM EQUATIONS

Compression Members

Because the proposed closed-form solution was developed using a deterministic approach, which does not account for uncertainty in estimation of applied load ratios, P_u/P_{na} , sensitivity was examined with variability in mechanical properties of steel (F_y and elastic modulus, E) and the magnitude of design loads (e.g., dead load, DL , and live load, LL).

Although uncertainty in geometric properties are present in the proposed equation, such as column length, L_c , and the radius of gyration, r , this effect was neglected with the assumption that compliance of standard fabrication tolerances specified in the *AISC Code of Standard Practice for Steel Buildings and Bridges* (AISC, 2016a) would not result in notable critical temperature changes. A comparison of the influence of each parameter (F_y , E , DL , and LL) on the variation in the critical temperature was calculated by considering reasonable upper and lower bounds of each variable. Each parameter was evaluated at the mean ± 1 standard deviation (std) that represents 68% confidence intervals. The mean ± 2 standard deviations (to represent a 95% confidence interval) were also reported. A normal distribution of each variable was assumed.

Statistical properties of the investigated variables are summarized in Table 2, based on work from Takagi and Deierlein (2007), who proposed the member strength equation for gravity columns at elevated temperature in *AISC Specification Appendix 4*. The mean values and coefficients of variation (CV) were determined from statistical data obtained by Ellingwood et al. (1980). The percentages

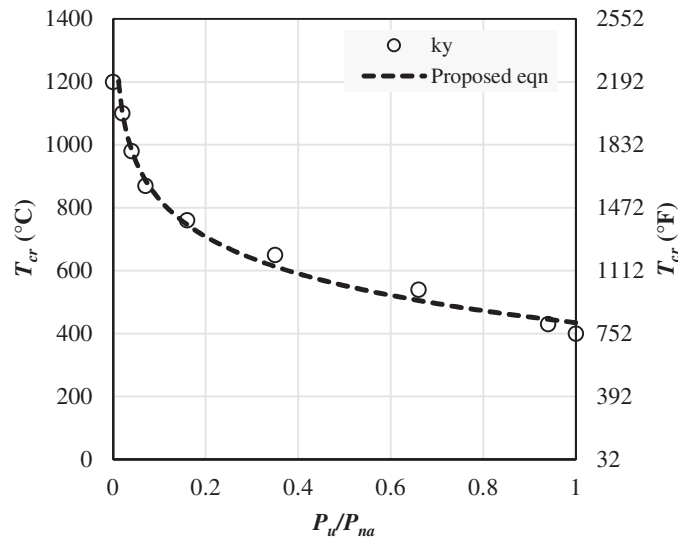


Fig. 6. Critical temperature versus load ratio relationship of tension members.

for *DL* and *LL* were obtained from load surveys using probabilistic load models. They represent the mean values of the unfactored design loads for dead and live loads relative to the nominal design loads in the American National Standard A58. The standard deviation (std) for each variable was calculated as the mean times the coefficient of variation (CV), as shown in Table 2. Ambient temperature values of F_y and E were used to calculate the mean and CV values due to a lack of statistical data on their high-temperature values.

A range of columns used in this study (W8×31, W14×90, and W14×211 with $F_y = 50$ ksi) were examined for sensitivity. The change in critical temperature due to uncertainty of 1 standard deviation is consistent across all compact column shapes, so the results presented represent all of the compact shapes listed above. Figure 7 shows the change in critical temperature for the W14×211 column with $L_c/r = 40$ and $L_c/r = 80$ due to uncertainty in F_y . The solid line

represents the critical temperatures determined using the proposed closed-form equation [Equation (1)]. The dashed lines represent the critical temperatures calculated with F_y adjusted by a positive and negative standard deviation. The uncertainty in the critical temperature estimated using the propose equation is more pronounced at lower L_c/r ratios and at higher load ratios where Euler buckling does not likely occur. At higher L_c/r levels, where elastic buckling of the column would dominate, the impact of a change in F_y , appears to be minimal and becomes negligible for L_c/r ratios of 120 and greater. At a load ratio (P_u/P_{na}) of 0.6, the uncertainty in estimated critical temperatures is about 20% at $L_c/r = 40$ and about 10% at $L_c/r = 80$ due to ± 1 std of F_y . These percentages represent the ratio of change in critical temperature due to uncertainty relative to the closed-form proposed equation without uncertainty.

Figure 8 shows the variation in estimated critical temperature for the W14×211 column with $L_c/r = 40$ and $L_c/r = 120$

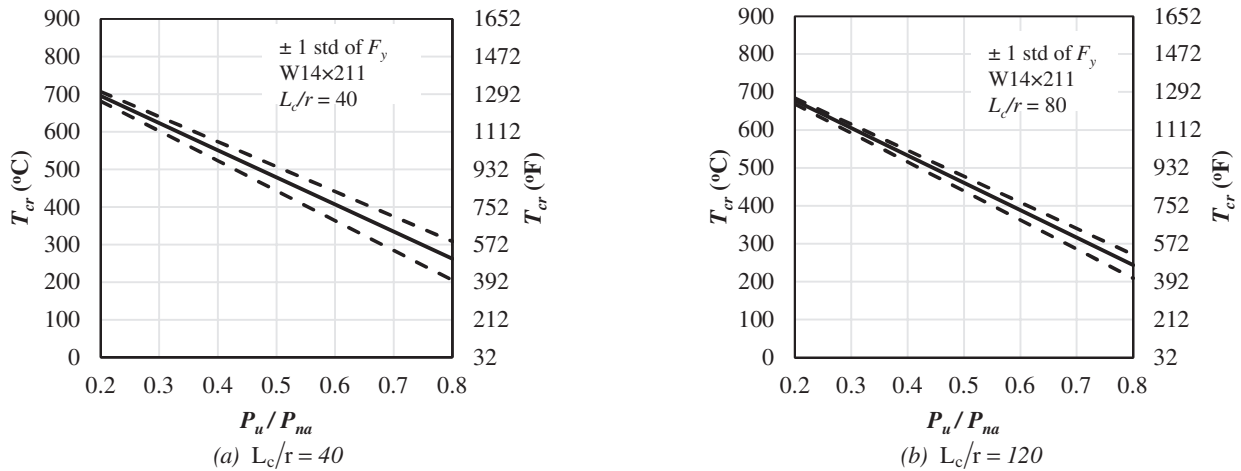


Fig. 7. Sensitivity of calculated critical temperatures of a W14×211 column due to uncertainty in F_y .

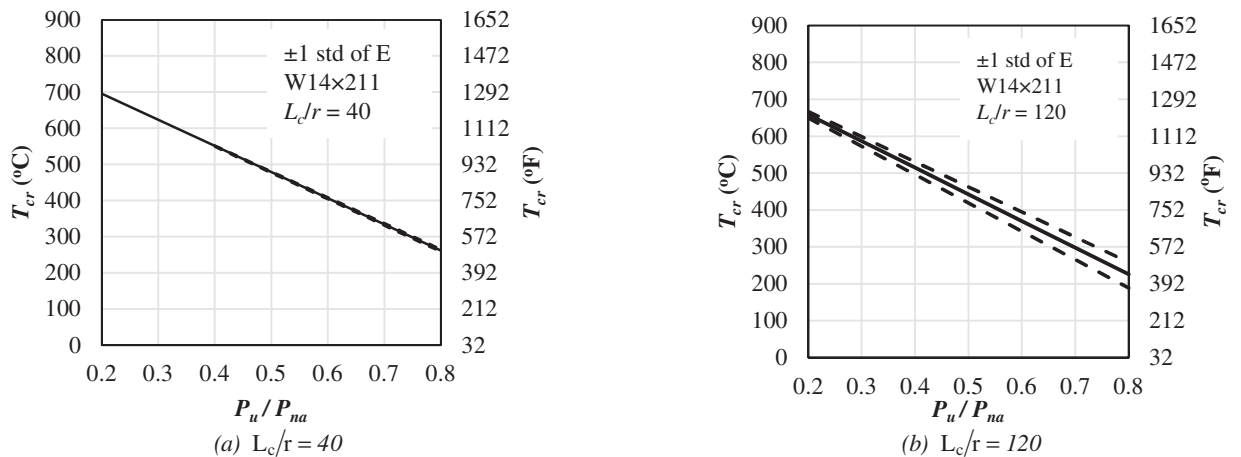


Fig. 8. Sensitivity of calculated critical temperatures of a W14×211 column due to uncertainty in E .

due to uncertainty in the elastic modulus, E , in the calculation of P_{na} . The uncertainty in estimated critical temperature is most pronounced at both higher slenderness and higher load ratios where elastic buckling likely governs. In this study, the maximum uncertainty is observed for slender columns ($L_c/r \geq 120$) and the applied load ratio of 0.8. For these columns, the uncertainty in critical temperatures can be as large as 30%. However, for stockier columns ($L_c/r \leq 40$), this uncertainty in critical temperatures associated with ± 1 std of E becomes very minor, less than 3%.

Sensitivity due to uncertainty in applied loads under fire conditions (P_u) was determined by considering three different DL/LL ratios selected based on engineering judgment. The first DL/LL ratio was 0.65, which was determined by assuming a dead load of 65 psf and a live load of 100 psf. The second DL/LL ratio of 1.3 was calculated using the same dead load of 65 psf but a live load of only 50 psf. The 65-psf dead load was selected based on the assumption of

50 psf for the composite slab plus 15 psf for superimposed dead loads such as ceilings and ductwork and piping for utilities. The live load values of 50 psf and 100 psf represent average and high levels of live loading, respectively. According to ASCE/SEI 7 (2016), 50 psf represents live loads for office spaces, while 100 psf represents lobbies and other assembly areas. The final DL/LL ratio that was used was 0.33. This ratio is given in the AISC *Specification* Section A1 Commentary (AISC, 2016b) as the ratio that results in the same reliability between the ASD and LRFD design methods. Using these ratios, the dead and live loads on the column were determined by assuming that the demand-to-capacity ratio for each column at ambient conditions is equal to 1.0 for the ambient load combination, $1.2DL + 1.6LL$. Converting to the fire load combination ($1.2DL + 0.5LL$), this equates to a P_u/P_{na} ratio of approximately 0.4, 0.5, and 0.6 for DL/LL ratios of 0.33, 0.65, and 1.3, respectively. Figure 9(a) shows the change in critical

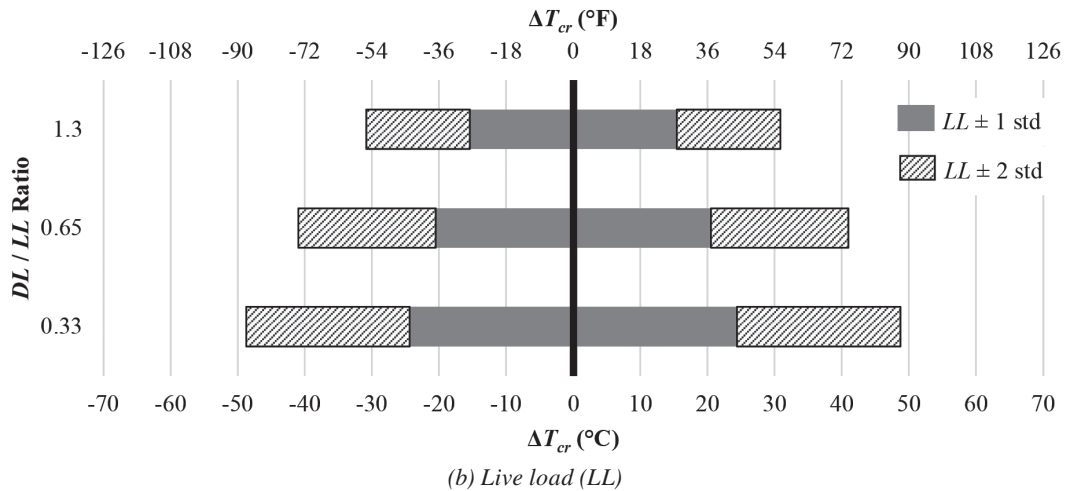
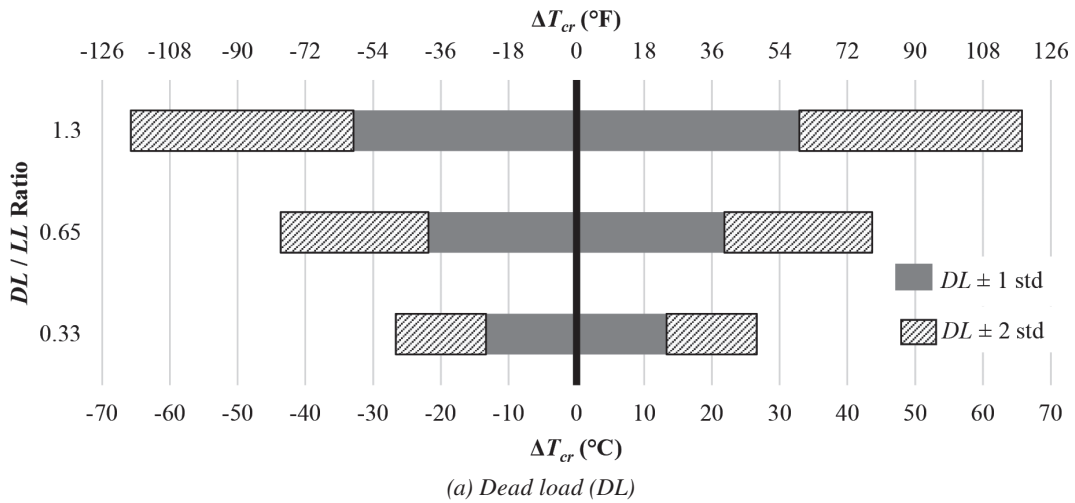


Fig. 9. Sensitivity of the change in critical temperature due to uncertainty. Note: ΔT_{cr} is presented (not T_{cr}); $\Delta T_{cr} (^{\circ}F) = 9/5[\Delta T_{cr} (^{\circ}C)]$.

temperature due to uncertainty in dead load, while Figure 9(b) represents the change in critical temperature due to live load uncertainty. These results show that critical temperatures are more influenced by a higher DL/LL ratio for dead load variability and a lower DL/LL for live load variability. These critical temperature changes (ΔT_{cr}) are independent of the L_c/r ratio of the column. The maximum change in critical temperature due to uncertainty of 1 standard deviation in DL and LL is 59°F and 44°F , respectively.

Tension Members

The same variables (F_y , DL , and LL) were studied for tension members to determine the sensitivity of the closed-form equation. There is no sensitivity in the equation to a change in modulus of elasticity (E). A $W14\times 22$ shape was chosen to demonstrate the sensitivity. Figure 10 summarizes the sensitivity by showing the change in critical temperature for ± 1 std and ± 2 std of each parameter, estimated using CV values in Table 2. The same DL/LL ratios of 0.33, 0.65, and 1.3 were also used. This comparison shows that the greatest change in critical temperatures is due to a change in the yield stress of the material. At 1 standard deviation, the change in temperature is -32°F to 29°F , and at 2 standard deviations, it is -68°F to 56°F . The variation in DL with a high DL/LL ratio produces the second highest sensitivity.

SUMMARY AND CONCLUSIONS

This paper presents the development of closed-form solutions to evaluate critical temperatures of axially loaded steel members exposed to fire. For compression members,

a total of 900 FEM models were analyzed in combination with various ranges of parameters, including five different wide-flange rolled shapes made of two American standard grades of structural steel, member slenderness ratios from 20 to 200, and applied load ratios varying from 0.1 to 0.9. Load ratios represent the axial demand at elevated temperatures, P_u , normalized by the nominal capacity at ambient temperature, P_{na} .

The parametric study indicates that the most influential parameters for critical temperature of columns are member slenderness and applied load ratios. A closed-form equation predicting critical temperatures of steel columns with these two factors is proposed based on curve-fitting of the FEM results using the three-dimensional linear polynomial model. With this equation, the load-bearing capacity of steel columns is approximately 40% of the ambient capacity at the ASTM E119 limiting temperature of 1000°F (540°C). At load ratios less than 0.6, the proposed equation accurately predicts critical temperatures determined using the high-temperature flexural buckling strength equation in AISC *Specification* Appendix 4, whereas it may overestimate critical temperatures (10% difference or greater) at load ratio greater than or equal to 0.6. The proposed equation also provides a conservative lower bound (16% lower on average) of the published test data for the specimens with load ratios greater than 0.3. This result considers column failure by flexural buckling at elevated temperature.

A critical temperature equation for tension members is also proposed using the logarithmic regression model for the case with tensile yielding only. This equation is essentially the same as an inverse relationship of the AISC

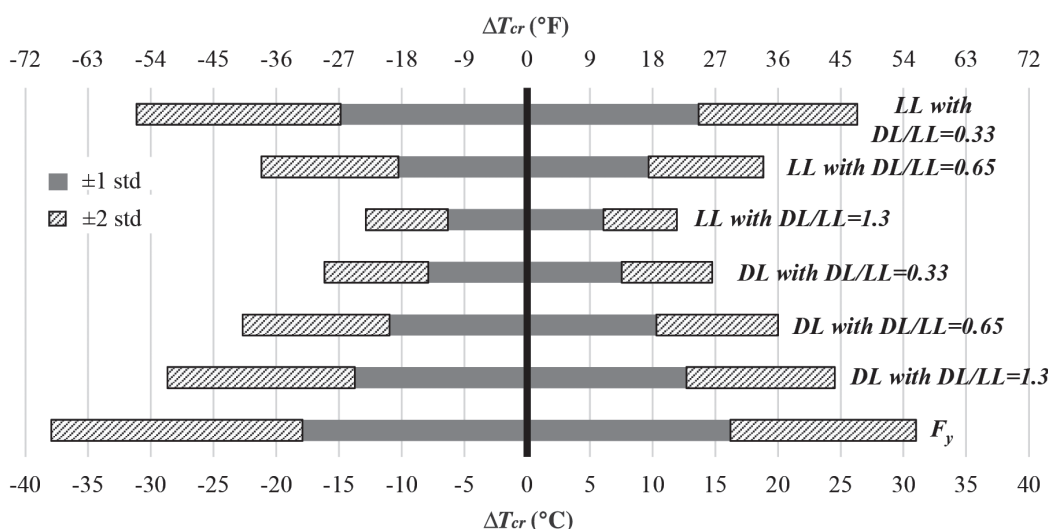


Fig. 10. Sensitivity of the change in critical temperature of tension members due to uncertainty in parameters. Note: ΔT_{cr} is presented (not T_{cr}); $\Delta T_{cr}(^\circ\text{F}) = 9/5[\Delta T_{cr}(^\circ\text{C})]$.

Specification temperature-dependent retention factors for yield stress.

A sensitivity study was performed to estimate the uncertainty in critical temperatures predicted using the proposed equations due to the variability in axial load ratios. The results show that these critical temperatures depend on the ambient temperature F_y and E as well as design loads (DL and LL). The variation in F_y is the most influential factor among other uncertain variables for critical temperatures of both compression and tension members. The influence of F_y uncertainty is apparent in stout columns with a low slenderness ratio. All results show that variations in critical temperature are relatively minor for uncertainty of 1 standard deviation, particularly for typical columns, which are assumed to have load ratios of approximately 0.6 and L_c/r ratios of approximately 40 to 60. Consideration of material sensitivity should be implemented for load ratios beyond 0.6.

The findings and equations from this study are limited to the range of parameters included in the numerical evaluation. Future studies will be conducted to further incorporate probabilistic analyses into the current deterministic approach, accounting for the effects of thermal restraints as well as thermal gradients through the section depth and along the member length.

ACKNOWLEDGMENT

Valuable comments and input on this work were provided by the AISC Committee on Specifications Task Committee 8, Design for Fire.

DISCLAIMERS

Certain commercial entities, equipment, products, software, or materials are identified in this paper in order to describe a procedure or concept adequately. Such identification is not intended to imply recommendation or endorsement by the National Institute of Standards and Technology, nor is it intended to imply that the entities, products, software, materials, or equipment are necessarily the best available for the purpose.

REFERENCES

Ali, F.A., Shepherd, P., Randall, M., Simms, I.W., O'Connor, D.J., and Burgess, I. (1998), "The Effect of Axial Restraint on the Fire Resistance of Steel Columns," *Journal of Construction Steel Research*, Vol. 46, pp. 305–306.

AISC (2016a), *Code of Standard Practice for Steel Buildings and Bridges*, ANSI/AISC 303-16, American Institute of Steel Construction, Chicago, Ill.

AISC (2016b), *Specification for Structural Steel Buildings*, ANSI/AISC 360-16, American Institute of Steel Construction, Chicago, Ill.

ASCE (2016), *Minimum Design Loads and Associated Criteria for Buildings and Other Structures*, ASCE/SEI 7-16, American Society of Civil Engineers, Reston, Va.

ASTM (2019), *Standard Methods of Fire Test of Building Construction and Materials*, ASTM E119-19, ASTM International, West Conshohocken, Pa.

BSI (2005), *UK National Annex to Eurocode 3. Design of Steel Structures. General Rules. Structural Fire Design*, BS NA EN 1993-1-2, United Kingdom.

Choe, L., Varma, A.H., Agarwal, A., and Surovek, A. (2011), "Fundamental Behavior of Steel Beam Columns and Columns under Fire Loading: Experimental Evaluation," *Journal of Structural Engineering*, Vol. 137, pp. 954–966.

Choe, L., Zhang, C., Luecke, W.E., et al. (2017), "Influence of Material Models on Predicting the Fire Behavior of Steel Columns," *Fire Technology*, Vol. 53, pp. 375–400, <https://doi.org/10.1007/s10694-016-0568-4>.

CEN (2005), *Eurocode 3: Design of Steel Structures—Part 1-2: General Rules—Structural Fire Design*, Standard EN 1993-1-2, European Committee for Standardization, Luxembourg.

Ellingwood, B., Galambos, T.V., MacGregor, J.G., and Cornell, C.A. (1980), "Development of a Probability-Based Load Criterion for American National Standard A58," National Bureau of Standards Special Publication No. 577, Washington, D.C.

Franssen, J.M., Schleich, J.B., Cajot, L.G., and Azpiazu, W. (1996), "A Simple Model for the Fire Resistance of Axially-Loaded Members—Comparison with Experimental Results," *Journal of Construction Steel Research*, Vol. 37, pp. 175–204.

Franssen, J.M. (2000), "Failure Temperature of a System Comprising a Restrained Column Submitted to Fire," *Fire Safety Journal*, Vol. 34, No. 2, pp. 191–207.

ICC (2009), *International Building Code*, International Code Council, Falls Church, Va.

Kim, S. and Lee, D. (2002), "Second-Order Distributed Plasticity Analysis of Space Steel Frames," *Engineering Structures*, Vol. 24, pp. 735–744.

Kruppa, J. (1979), "Collapse Temperature of Steel Structures," *Journal of the Structural Division*, ASCE, Vol. 105, No. ST9, September.

Milke, J.A. (2016), "Analytical Methods for Determining Fire Resistance of Steel Members," In: Hurley M.J. et al. (eds.), *SFPE Handbook of Fire Protection Engineering*, Springer, New York, N.Y., https://doi.org/10.1007/978-1-4939-2565-0_53.

- Neves, I.C. (1995), "The Critical Temperature of Steel Columns with Restrained Thermal Elongation," *Fire Safety Journal*, Vol. 24, pp. 211–227.
- Rubert, A. and Schaumann, P. (1988), "Critical Temperatures of Steel Columns Exposed to Fire," *Fire Safety Journal*, Vol. 13, pp. 39–44.
- Sauca, A., Zhang, C., Seif, M., and Choe, L. (2019), "Axially Loaded I-Shaped Steel Members: Evaluation of Critical Temperature Using ANSI/AISC-360 Appendix 4 and Finite Element Model," *Proceedings of the Annual Stability Conference*, Structural Stability Research Council, St. Louis, Mo., April 2–5.
- Smith, M. (2009), *ABAQUS/Standard User's Manual, Version 6.9*, Simulia, Providence, R.I.
- Takagi, J. and Deierlein, G.G. (2007), "Collapse Performance Assessment of Steel-Frames Buildings under Fires," John A. Blume Earthquake Engineering Center Technical Report No. 163.
- Vassart, O., Zhao, B., Cajot, L.G., Robert, F., Meyer, U., and Frangi, A. (2014), "Eurocodes: Background & Applications Structural Fire Design," *JRC Science and Policy Reports*, European Union.
- Vila Real, P.M.M., Lopes da Silva, N.L.S., and Franssen, J.M. (2007), "Parametric Analysis of the Lateral—Torsional Buckling Resistance of Steel Beams in Case of Fire," *Fire Safety Journal*, Vol. 42, pp. 461–524.
- Wang, P., Wang, Y.C., and Li, G.Q. (2010), "A New Design Method for Calculating Critical Temperatures of Restrained Steel Column in Fire," *Fire Safety Journal*, Vol. 45, pp. 349–360.
- Zhang, C., Choe, L., Seif, M., and Zhang, Z. (2015), "Behavior of Axially Loaded Steel Short Columns Subjected to a Localized Fire," *Journal of Constructional Steel Research*, Vol. 111, pp. 103–111.